LA-UR-78-2258

CONF-780575--3

MASTER

TITLE: NONLINEAR CHARACTERISTICS OF CYCLOTRON WAVES IN AN ARA CONFIGURATION

MASTER

AUTHOR(S): R. J. Faehl, W. R. Shanahan, and B. B. Godfrey

SUBMITTED TO: Proceedings of the Third International Conference on Collec ive Methods of Acceleration

los alamos
scientific laboratory
of the University of California
LOS ALAMOS, NEW MEXICO 87545

An Affirmative Action/Equal Opportunity Employer

Intense Particle Beam Theory Group (T-15)

Form No. 836
St. No. 2629
1/75

UNITED STATES
ENERGY RESEARCH AND
DEVELOPMENT ADMINISTRATION
CONTRACT W-7405-ENG. 36

NONLINEAR CHARACTERISTICS OF CYCLOTRON WAVES IN AN ARA CONFIGURATION

R. J. FAEHL, W. R. SHANAHAN, AND B. B. GODFREY
University of California, Los Alamos Scientific Laboratory, Theoretical Division, Los Alamos, New Mexico 87545

The Autoresonant Accelerator (ARA) offers great promise for collective ion acceleration provided large amplitude cyclotron waves can be generated with long coherence scales and controllable propagation characteristics. Numerical simulations have been performed to examine cyclotron wave growth in a helical slow-wave structure. No inhibition of growth was observed, short of an intrinsic space charge limitation. Extraction of such waves from the amplifying section through realistic terminations has been performed. The radial structure and propagation of these large, extracted cyclotron waves has been studied and comparisons with linearized waves have been drawn. The effect of nonlinear wave properties on ARA designs are presented.

I. INTRODUCTION

Ion acceleration in collective wave fields of relativistic electron beams has been studied energetically in recent years. The Auto-Resonant Accelerator (ARA), which utilizes a slow cyclotron mode, is probably the best analyzed and furthest developed of such collective wave schemes. In these conceptually simple schemes, ions are trapped in a beam supported wave, which is then accelerated in some fashion. There are implicit assumptions here, however, namely that nonlinear waves (a) remain coherent for long distances and times and (b) behave, at least approximately, like linear waves. These fundamental questions have motivated us to study finite amplitude cyclotron waves such as are needed in the ARA. We have studied the nonlinear wave characteristics with emphasis on radial wave structure, field strength, and possible deviations from linear dispersion. Large two-dimensional particle simulations were used to grow waves self-consistently and then follow their subsequent propagation. These results have been augmented by numerical studies of radially inhomogeneous linear theory and analysis of nonlinear waves.

The overall structure of this paper is as follows. Linear theory and the equations from which it is derived are examined briefly. Origin of the axial electric field, the component responsible for ion acceleration, is discussed. Also, qualitative examination of the equations suggests possible nonlinear effects. The simulations themselves are then described. Finally, simulation results are given in which slow cyclotron waves are grown from small amplitude signals and stable propagation is observed over modest scale lengths. Analysis of the simulations is performed to obtain data which can be compared directly with linear theory.

II. LINEAR THEORY AND NONLINEAR CYCLOTRON WAVES

Before discussing "nonlinear waves", it is proper to define what we mean by "nonlinear". The term is used in this context simply to distinguish finite amplitude waves from the results of first-order perturbation analysis. This is complicated since unique equilibrium conditions make even linear analysis of unneutralized relativistic electron beams nontrivial. A brief analysis of the linear equations shows this clearly.

Relativistic electron beam equilibrium during vacuum propagation in a smooth-walled drift tube requires a large, external axial magnetic field, B_z. Since the beam is unneutralized, significant radial electric and azimuthal magnetic fields are present with magnitudes determined by total beam current, beam and drift tube dimensions, and radial density distribution. For these to be self-consistent, the beam must rotate, giving a zero-order v_θ. Finally, since there are large equilibrium potentials, injection of even a monoenergetic beam into a finite radius drift tube results in radial variations in γ, given by

$$mc^2(\gamma_0 - 1) = mc^2(\gamma(r) - 1) - e\phi(r) \quad , \quad (1)$$

where $\gamma = [1 - (v/c)^2]^{-1/2}$ and ϕ is the electrostatic potential. Linearization around a <u>self-consistent</u> beam equilibrium leads to equations which, to the best of our knowledge, do not possess closed-form solutions. Consequently, analytic efforts have often neglected beam rotation, density inhomogeneity, and/or radial γ-variations. As we show below, the consequences can be significant vis-a-vis collective ion acceleration.

The dispersion of beam cyclotron waves can be quite accurately described with a reduced set of linearized cold fluid and field equations, which for azimuthally symmetric modes ($m = 0$) are

$$\frac{\partial \tilde{p}_r}{\partial t} + v_z \frac{\partial \tilde{p}_r}{\partial z} - 2v_\theta \frac{\tilde{p}_\theta}{r} = -\frac{e}{m}(\tilde{E}_r + \tilde{v}_\theta B_z - v_z \tilde{B}_\theta) \qquad (2)$$

$$\frac{\partial \tilde{p}_\theta}{\partial t} + v_z \frac{\partial \tilde{p}_\theta}{\partial z} + v_\theta \frac{\tilde{p}_r}{r} = -\frac{e}{m}(\tilde{E}_\theta + v_z \tilde{B}_r - \tilde{v}_r B_z) \qquad (3)$$

$$\frac{\partial \tilde{n}}{\partial t} = -\frac{\partial \tilde{n} v_z}{\partial z} - \frac{1}{r}\frac{\partial}{\partial_r} r\, n_0 \tilde{v}_r \qquad (4)$$

$$\frac{\partial^2 \tilde{A}_i}{\partial t^2} - c^2 \frac{\partial^2 \tilde{A}_i}{\partial z^2} - c^2 \frac{1}{r}\frac{\partial}{\partial r} r \frac{\partial \tilde{A}_i}{\partial r} = 4\pi ec(n_0 \tilde{v}_i + \tilde{n} v_i) \qquad (5)$$

where tildes refer to perturbed quantities, $v_r = 0$, $\tilde{p}_i = \gamma_0 \tilde{v}_i$, $i = r,\theta$, and A is the vector potential, such that $\tilde{B} = \nabla \times \tilde{A}$. Numerical solution of the full fluid and field equations on self-consistent equilibria provide confidence in the viability of (2-5) for modeling cyclotron waves.[6,7] Aside from their utility in deriving dispersion relations, this reduced set can yield information directly about nonlinear waves.

In writing the model equations (2-5), the $\tilde{p}_z$ and $\tilde{E}_z$ equations were omitted. Although they could be included for the sake of accuracy, they effectively decouple from cyclotron waves of interest to ARA. In fact, they arise almost as by-products. The v_r and v_θ induced motions characterize the wave, leading to periodic radial modulations of the beam. Figure 1, taken from a wave growth simulation, clearly shows this. In Fig. 1(a), the configuration space (r - z) of the beam exhibits this beam modulation after a section of convective wave growth.

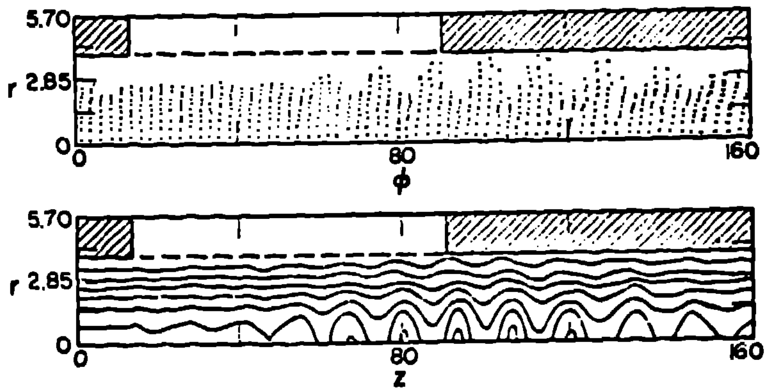

Fig. 1. Convectively grown cyclotron wave in particle simulation, (a) configuration space (r - z) and (b) constant contours of electrostatic potential, ϕ.

Figure 1(b) shows the corresponding constant contours of ϕ, the electrostatic potential. The potential troughs are associated with the modulations. This is the source of the E_z field which traps and accelerates the ions; the radial modulation causes density compressions and rarefactions. Thus, the cyclotron wave always possesses some E_z field, but its magnitude is determined by the depth of radial modulation. To be more precise, it is the radial integral of the density modulation which determines E_z, and this depends on the structure of v_r, since $\delta r \approx v_r/(\Omega/\gamma)$, $\Omega = eB_z/mc$. If the radial perturbation is distributed broadly across the beam, the integrated density modulation will be greater than if it were, say, localized on the surface. Since there is only a finite beam-to-wall separation, the magnitude of modulation on the outside of the beam is limited. Maximizing the axial electric field, therefore, depends sensitively on the radial eigenmodes.

Other information deducable from Eqs. (2-5) is more qualitative. Examination of the first order equations shows the terms neglected in this order, but which in general need not be small. A prime example is the radial convective term, $v_r(\partial p_i/\partial_r)$, $i = r,\theta$. These terms are clearly not first order. However, when the waves become finite, perturbation schemes become dubious and actual magnitudes must be considered. In this case, lack of an axially homogeneous ($k = 0$) v_r component indicates that, for large waves at k_0, the convective terms contribute most strongly at $2k_0$, the spatial second harmonic. (Since the $2k_0$ contribution is not resonant, however, only forced oscillations are induced.) More directly applicable terms are those involving v_z. In the reduced equations, only the $k = 0$ component was retained. The self-field $B_\theta(k = 0)$ can be quite large, however, so finite values of $v_z(k = k_0)$ can contribute significantly to the k_0 mode. While one can argue that these should be included in linear theory, v_z is coupled nonlinearly with wave amplitude, through

$$\tilde{v}_z \cong c(\gamma^2 - 1 - \tilde{p}_r^2 - \tilde{p}_\theta^2)^{1/2}/\gamma \quad . \tag{6}$$

This nonlinear term can directly alter the cyclotron dispersion. Linear results are of little value in estimating $\tilde{v}_z$ since there is no guarantee á priori that the nonlinear ratio of wave quantities remains fixed. One of our primary objectives, in fact, is to determine the relative magnitudes of nonlinear wave quantities. To do this, more powerful numerical tools are required.

III. DESCRIPTION OF CYCLOTRON WAVE GROWTH SIMULATIONS

The study of relativistic slow cyclotron waves requires self-consistency. Two-dimensional relativistic particle simulations were therefore conducted to amplify small amplitude cyclotron-like perturbations. The large amplitude extracted signals were then allowed to propagate for moderate distances in a smooth-walled guide. A more complete discussion of the cyclotron wave growth has been reported elsewhere,[7] but a brief outline will now be given to place that work in perspective.

Wave growth in a helical slow wave structure has been widely employed for many years, for example, as the basis for traveling wave tubes. The principle of operation is that in a helix waveguide structure, the phase velocity of the electromagnetic mode is reduced to $V_{ph} \cong c \sin \psi$, where ψ is the helix pitch angle. It is, in fact, lowered to the point where resonance with a slow beam mode is achieved. Only slow modes can be resonant since, by definition, they alone possess phase velocities slower than the medium velocity, in this case $v_0 \approx c$. In traveling wave tubes, the beam mode is a Langmuir wave. ARA applications call for unstable growth of the slow cyclotron wave, however. This mode is quite dissimilar from the space charge wave. Previous theoretical and experimental experience was therefore inapplicable. This led to a number of unpleasant surprises in the simulations before certain fundamentals of electrical engineering were rediscovered and successful stable amplification was achieved.

Figure 2 depicts the simulation configuration used in these studies. A sheath helix with pitch angle ψ and radius R_H, illustrated with the dashed line in the figure,

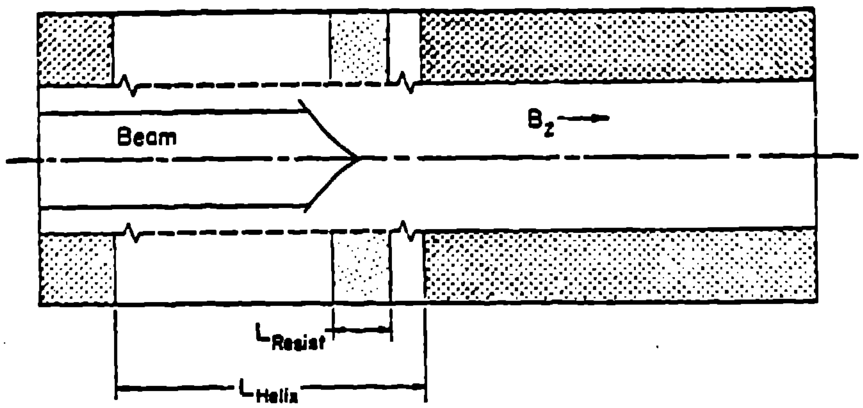

Fig. 2. Schematic representation of the simulation configuration employed to grow cyclotron wave.

was attached to perfectly conducting flanges on either end, shown as crosshatching. An outer conducting wall with radius R_W existed outside the helix. The relativistic electron beam was injected on the left simulation boundary and propagated to the right, downstream boundary, where it was "smoothly" extracted. Once the space charge fields reached the grounded helix, they induced a charge flow on it. This "charging current" is quite physical and in a non-resistive helix, it rang for an unacceptably long period. More gentle risetimes would have ameliorated this condition, for helix dispersion eventually smooths the charging pulse. Although the helix current smoothed, however, the residual current flow resulted in a strong, finite width diamagnetic region. The total B_z field experienced by the beam was therefore discontinuous at the flange/helix boundaries. This stationary discontinuity excited zero-frequency cyclotron waves with wavenumber $k \cong \Omega_0/\gamma_0 v_0$. These waves did not interfere with growth of the coupled helix/cyclotron waves, but beating of the two finite amplitude cyclotron modes yielded a potential distribution unsuitable for long-term trapping. Removal of the helix current without disturbing helix charge distributions was found to be highly desirable, and accomplished in the simulations, as in the laboratory, by terminating the helix with matched impedances. After the initial transients decayed away, the current and charge distributions were quiescent and suitable for introduction of a small amplitude signal at the most unstable frequency upstream of the helix. Our "generator" was directly tied to the helix, but other more physical antennas have been examined. When the signal generator was "turned on", steady cyclotron wave amplification occurred, in close agreement with linear theory. To prevent oscillation, rather than amplification, large volumetric resistances were added outside the helix at the far end of the growth section. These were sufficiently large that they inhibited amplification, but such magnitudes were required to prevent oscillation. After the resulting large amplitude cyclotron wave reached the end of the helix, it was found to propagate into the smooth-walled drift tube with only nominal (10-20%) attenuation of the wave.

IV. DISCUSSION AND ANALYSIS OF NUMERICAL CALCULATIONS

The model configuration described above was successfully employed to grow large amplitude cyclotron waves. Since growth is due to coupling with the helical waveguide mode, however, the finite amplitude wave possessed a different radial structure from a stable cyclotron wave. Relaxation toward a stable configuration is thus expected after the wave leaves the growth section. This is, in fact, the dominant behavior observed in simulations. A small fraction of the wave energy is nevertheless converted into high frequency noise. This noise seems to couple into resonant TE and TM wave guide modes with moderate efficiency. These are only tentative conclusions, since there are indications that the coupling may be enhanced by purely numerical effects. Even if the simulations overestimate the magnitude of electromagnetic noise, however, the combination of high frequency with incoherence in this field make it unlikely to interfere with the cyclotron accelerating fields. The low frequency field itself showed only weak attenuation or loss of coherence as it propagated for distances of order $L = 100\ c/\omega_p$ beyond the growth section. The only wave coupling effect observed was a tendency toward generation of harmonics, which never amounted to more than a few percent of the primary wave energy.

Demonstration of long coherence lengths for nonlinear cyclotron waves was accomplished with the numerical simulations. Beyond this, however, a primary objective was to characterize the finite amplitude wave state. How then should a nonlinear wave be characterized? Linear waves are completely described once a dispersion relation and the eigenfunctions are determined. The situation is much more complicated for finite amplitude waves. For one thing, linear superposition of modes is no longer strictly valid; a non-zero coupling between all modes exists in general. Therefore, while it is still important to determine the relation between ω and k, i.e., the dispersion, one also needs to specify the spectrum. Spectral characteristics are a self-consistent aspect of a nonlinear wave state. The radial wave structure in our case is also a valid indicator, in so far as it can be compared with a linear eigenfunction. As mentioned earlier, it can be directly correlated with the E_z field of the wave. Finally, linear theory allows us to predict ratios of eigenfunctions, for instance, $v_r|_{max}/E_z|_{max}$. Similar ratios can be determined directly from sim- tions. In this fashion, the degree to which nonlinear waves resemble linear ones can be inferred quantitatively. To make these concepts more concrete, we will consider a typical simulation.

A series of simulation calculations was performed in a geometry similar to that in Fig. 2. In units of c/ω_p*, the helix and the inner flange radii were $R_H = 3.8$, the outer flange radius was $R_W = 5.7$, and the beam radius, $R_B = 2.65$. This last dimension corresponds to a Budker parameter of $\nu = 1.75$, or 30 kA. The helix extended from $z = 15.0$ to 115.0, with a pitch angle $\psi = -15°$. The helix was excited directly at $z \approx 30$, giving a total growth length $L_{grow} = 85$. For these conditions, the growth rate was $\Gamma = 0.020\ \omega_p$ and the group velocity $v_{gr} \approx 0.6$ c, giving almost 3 e-foldings, in the absence of resistive terminations. These simulations were designed for conservative performance, with a maximum power amplification of only about a factor of 260. In fact, addition of various resistive elements to inhibit feedback shortened the effective growth length, so that the observed amplification factor was on the order of 130. Our purpose here was not maximum amplification; in specifically designed wave growth simulations, amplification factors almost 10 times larger have been measured.[7] The

*For comparison purposes note that when $n_o \cong 3 \times 10^{11}$ cm^{-2}, $c/\omega_p \cong 1$ cm.

large amplitude cyclotron waves which were grown, however, proved very suitable for studying the nonlinear characteristics.

The magnitude of the E_z field on axis is plotted in Figure 3, as a function of axial position. The electric field is observed to reach its maximum value near the end of the helix. More significant, however, is that, while some fluctuations in amplitude are observed, the average field of the extracted wave is only about 10% lower than the peak.

The E_z values shown in Fig. 3 were obtained by setting numerical "probes" at various positions along the axis. Figure 4 shows a typical "probe" trace, near the end of the growth section, and its associated power spectrum. The dashed line indicates the frequency expected from linear theory for this configuration. There is virtually no detectable frequency shift, even though the magnitude is over 2×10^5 V/cm, assuming $n_0 = 10^{12}$ cm^{-3}. Since this probe was still within the region dominated by the linear helix, this is perhaps not surprising. Figure 5, however, compares that power spectrum with one obtained almost 90 c/ω_p further down the propagation path, well beyond the helix. Although the total noise content at high frequencies is quite different, the low frequency cyclotron signal is hardly affected at all.

With the aid of computer generated movies, a point of constant phase can be observed directly. The phase velocity of finite amplitude waves determined in this fashion was remarkably close to that of infinitesimal linear waves. As an example, a series of wave crests were followed for a distance $L = 50\ c/\omega_p$ and times on the order of $t = 300\ \omega_p^{-1}$. Wave modulation was such that

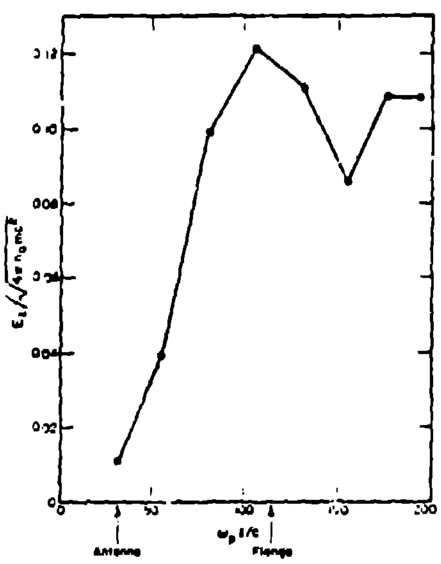

Fig. 3. E_z as a function of axial position, z; $r = 0.35\ c/\omega_p$, $R_B = 2.65$, $R_H = 3.8$, $R_W = 5.7/3.8$, $\psi = -15°$, $eB_o/mc = 2.0\ \omega_p$, $L = 200\ c/\omega_p$, $L_{grow} = 100\ c/\omega_p$.

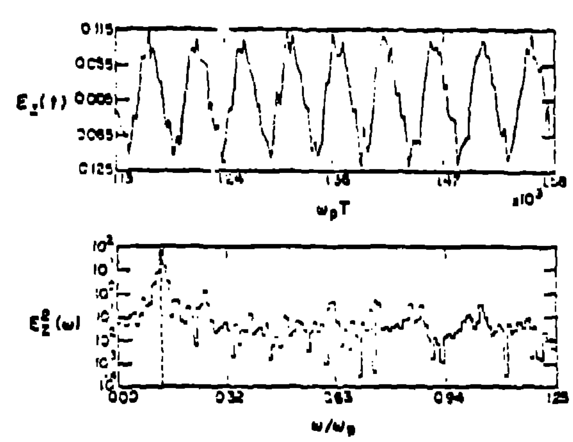

Fig. 4. (a) Typical E_z "probe" trace; r = 0.35, z = 106; (b) Power spectrum derived from probe trace. Dashed line indicates frequency of original antenna signal.

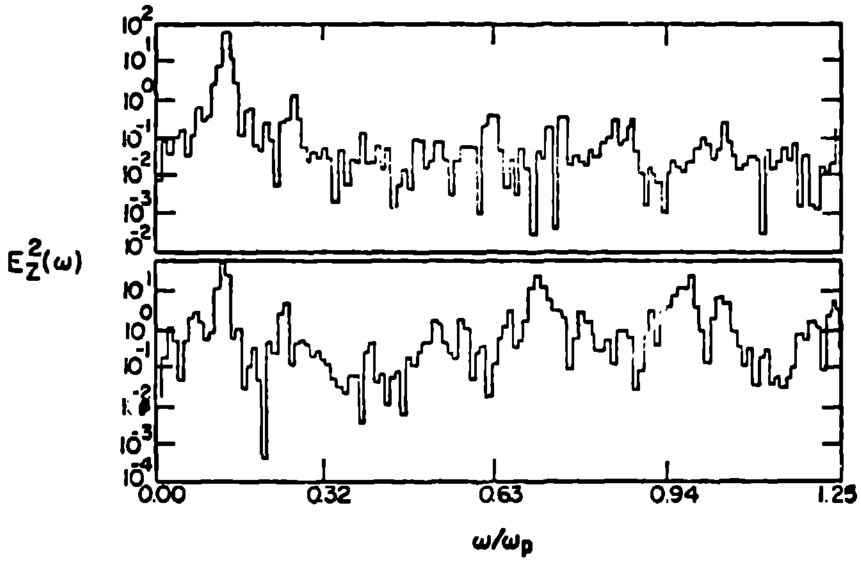

Fig. 5. Comparison of E_z power spectra at z. (a) z = 106 and (b) z = 193. Enhanced high frequency components at z = 193 may be due to numerical effects.

$\Delta r/R_B = 0.23$. (The beam-to-wall separation for this calculation corresponded to $\Delta r/R_B = 0.43$). The average phase velocity was measured to be $V_{ph} = 0.275$ c, while linear theory predicted $V_{ph} = 0.269$ c.

One of the few nonlinear spectral effects observed so far has been harmonic generation. This is registered to varying degrees on probes of E_z, B_θ, and E_θ fields, and seems to be correlated with the wave magnitude. The specific origin of this apparent nonlinearity has not yet been identified but is under investigation.

Figure 6 shows the beam envelope under typical conditions of steady cyclotron wave amplification. Radial beam modulations increase through the growth section, but are not attenuated on leaving it. In fact, they increase

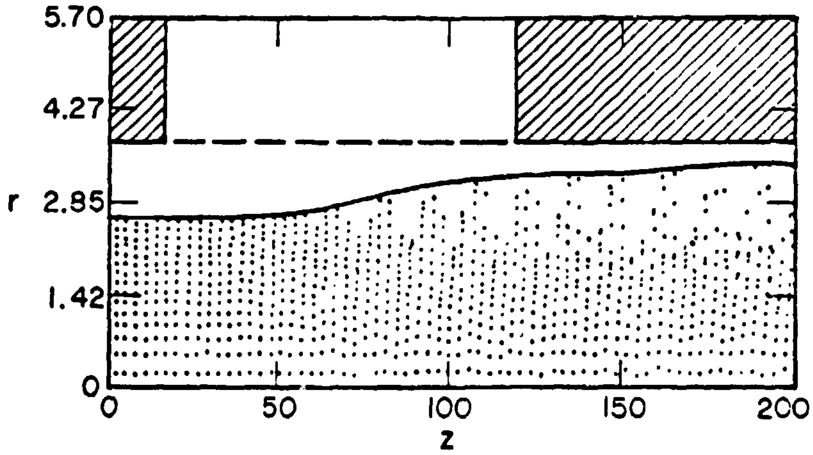

Fig. 6. Typical beam envelope in a wave growth run. Growth section extends from z = 15 to z = 115.

to somewhat larger values. Surprisingly, this behavior is explicable on the basis of inhomogeneous linear theory. Figure 7 shows the radial eigenfunctions for v_r derived on self-consistent radial profiles, with the same wavelength. These are related to the radial modulation by $\Delta r = \tilde{v}_r/(\omega - kv_0)$. Figure 7(a) depicts the radial velocity structure within the growth section; the frequency is $\omega = 0.124 \pm 0.020i\ \omega_p$. In Fig. 7(b), we show the eigenfunction under identical conditions, except that a smooth waveguide wall is at the helix radius; for constant frequency, the relative wavenumber shift is less than 1%. Both scales are normalized to the maximum value of E_z. Since Fig. 3 indicated that the E_z magnitude did not decrease significantly, it is evident that the radial modulation must increase substantially as the node relaxes toward its stable configuration.

We have repeatedly referred to inhomogeneous linear theory. The reason is well illustrated by the above example. To obtain the expected ratio, linearization was

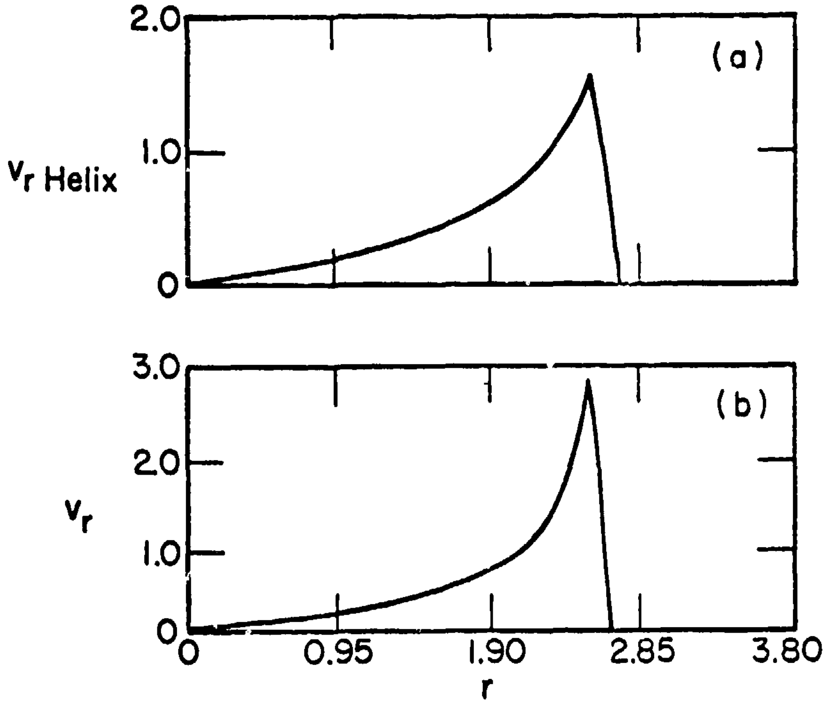

Fig. 7. Comparison of linear eigenfunctions of v_r derived numerically on a self-consistent equilibrium, $R_B = 2.65$, $\Omega_o = 2.0\ \omega_p$. (a) v_r versus r within growth section, $R_H = 3.8$, $R_W = 5.7$, $\psi = -15°$, $\omega = 0.124 \pm 0.020i\ \omega_p$, $k = 0.46\ \omega_p/c$; (b) v_r versus r in smooth-walled waveguide, $R_W = 3.3$, $\omega = 0.122\ \omega_p$, $k = 0.46\ \omega_p$.

performed around the radially inhomogeneous equilibrium. If the same calculation is conducted, except with a constant, averaged value of γ, i.e.,

$$\langle\gamma\rangle = \int_0^{R_B} \gamma\ dr/R_B \quad ,$$

qualitatively and quantitatively different eigenfunctions result. Figure 8 gives a comparison between the v_r and E_z eigenfunctions computed with $\langle\gamma\rangle$, Figs. 8(a,b) and those with $\gamma(r)$, Figs. 8(c,d). The difference is quite significant, for it indicates that, if linear theory is relevant to finite amplitude waves, over 4 times the density modulation is required to induce a given E_z magnitude than would be expected on the basis of the simpler $\langle\gamma\rangle$ analysis. Since the beam modulation is effectively limited to the beam-to-wall separation, this implies relatively small upper limits on the obtainable wave acceleration fields. Although the magnitude is still large compared with conventional fields, it is much smaller than originally anticipated. The self-consistent equilibrium employed here depends on a specific current distribution, of course, and this is certainly not unique.

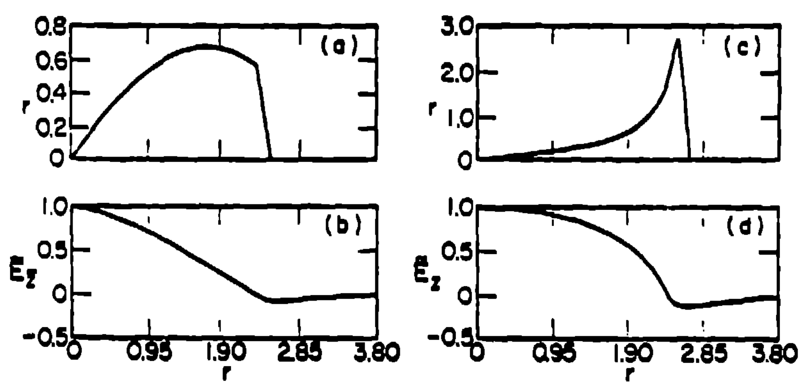

Fig. 8. Comparison of v_r and E_z linear eigenfunctions, $R_B = 2.65$, $R_W = 3.8$, $k = 0.46\,\omega_p/c$. (a) v_r versus r derived from equilibrium with $\langle\gamma\rangle = 4.9$, (b) E_z versus r, same as (a); (c) v_r versus r derived from self-consistent equilibrium, $\gamma(R_B) = 5.8$, $\gamma(0) = 4$, (d) E_z versus r, same as (c).

Tailoring the radial current distribution may yield more propitious field/modulation ratios. The important point is that linear theory at least should be based upon realistic, not idealized, beam states.

Eigenfunctions of the radial velocity were also compared with linear theory. These were obtained numerically by measuring the root-mean-square radial velocity of the beam at various axial slices as a function of the original stream lines, i.e.,

$$\langle v_r(r_0)\rangle = \left(\int_0^T v_r^2(r_0)dt/T\right)^{1/2} \quad .$$

The time interval for averaging was chosen large enough so that uncertainties in quantities at the desired wave frequency were less than 2%. Figure 9 shows the linear

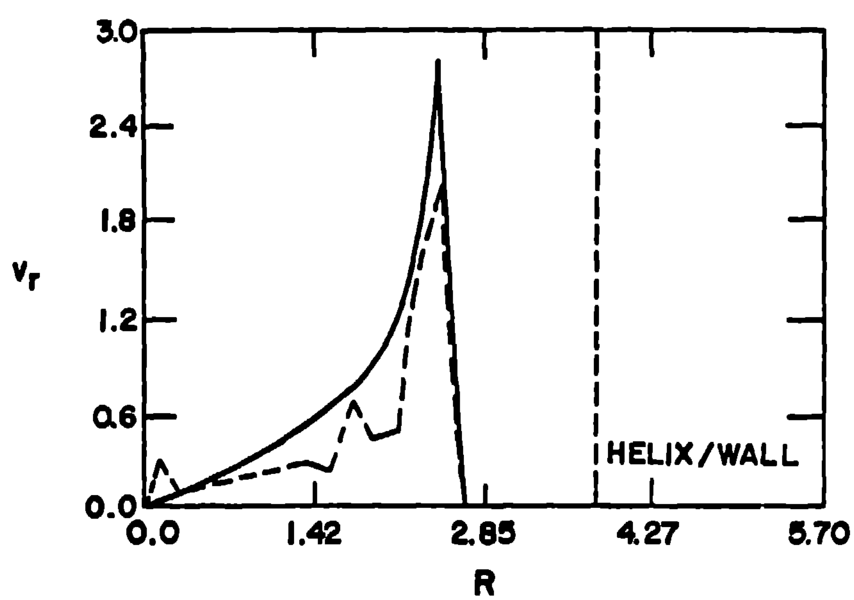

Fig. 9. Comparison of v_r linear eigenfunction (solid line) with RMS $v_r(r_o)$ derived from simulation (dashed line), $R_B = 2.65$, $R_W = 3.8$, $\delta r/R_B = 23\%$.

eigenfunction as a solid line, and the nonlinear as a dashed line, both normalized to the axial E_z magnitude. The structure is qualitatively the same, though the nonlinear wave exhibits less modulation. This is significant in that it indicates less modulation is required to produce a given E_z-field on axis. Compared with Fig. 8, however, it is apparent that inhomogeneous linear theory is more applicable to nonlinear waves than is simple linear theory.

The ratio of beam modulation to induced axial electric field is a very important accelerator parameter, due to finite beam/wall separation. Simulation derived values of $(\Delta r/E_z)_{max}$ are plotted in Fig. 10 as a function of z. It is clear that the ratio approaches the inhomogeneous linear values in both the unstable growth section and the stable propagation section.

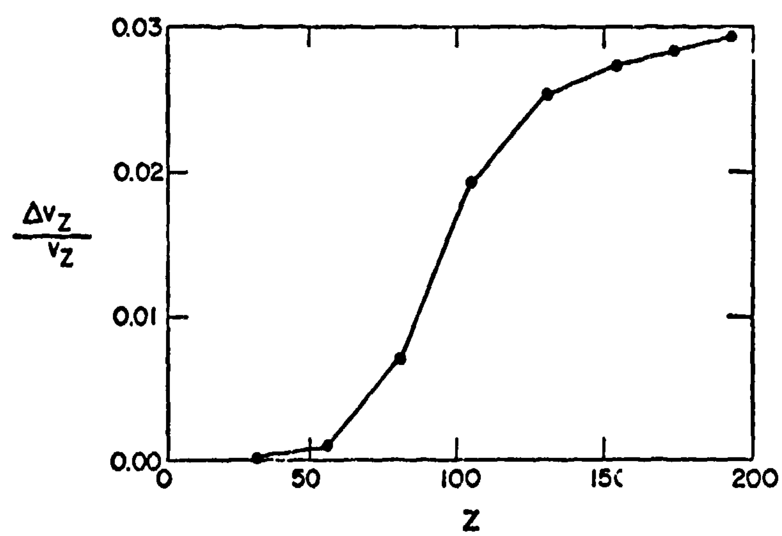

Fig. 10. Tabulated estimate of v_z shift as a function of z using Eq. (7) and simulation data, for parameters of Fig. 3.

Finally, note that finite transverse oscillations occur at the expense of the original beam energy, which was predominantly longitudinal. A simple model for the effect on longitudinal motion is

$$v_z(r_0) = c[\gamma_0^2(r_0) - 1 - p^2(r_0)]^{1/2}/\gamma_0(r_0) \quad . \tag{7}$$

Since we measured the RMS eigenfunctions of p_r, (7) can be estimated directly. Figure 10 shows the relative mean change in v_z as a function of z, for a typical wave growth/propagation simulation, with $\delta_r/R_B \lesssim 23\%$. This v_z not only induces frequency modulations through terms like $v_z B_\theta$ in Eq. (2), but also in the basic doppler shift, kv_z. If frequency shifts on the order of $k\Delta v_z$ are not compensated by wavelength shifts, the nonlinear phase velocity should have been reduced. Phase velocity changes of this size would have been seen in simulation movies, however, but the measured values, as discussed above, were not reduced. It is not clear at this time why such effects have not been observed in the simulations.

V. CONCLUSIONS

Cyclotron waves suitable for use in an Autoresonant Accelerator have been self-consistently grown to nonlinear levels in numerical simulations, and thereafter propagated for moderate distances without significant attenuation. While the investigation of these nonlinear wave states has not been completed yet, certain important observations can still be made.

The primary conclusion must be that cyclotron waves possessing relative radial modulations of 20% or less are not violently unstable, and in fact exhibit coherence lengths at least on the order of the simulations, i.e., $\Delta L \cong 10^2\ c/\omega_p$. Larger amplitude waves will be simulated in the near future. Comparisons with inhomogeneous linear theory revealed quantitative differences in nonlinear waves but no qualitative changes.

Finite amplitude cyclotron waves were also found to be highly localized on the beam surface, which is consistent with inhomogeneous linear theory. The interior of the beam does not "actively" participate in the oscillation. Therefore, a relatively large radial surface modulation, much larger than simple linear theory predicted, is needed to produce a given magnitude field on axis. Previous work has shown that an upper limit on the amplitude is that the total potential, equilibrium plus wave, must not exceed the space charge limit, roughly

$$\phi_{total} \lesssim (mc^2/e)(\gamma_0 - \gamma_0^{1/3}).$$ [7]

This in turn limits both the allowable beam-to-wall separation and the radial modulation. Although nonlinear cyclotron waves are not quite so surface-peaked as linear ones, the linear picture is still qualitatively correct. If these results prove to be valid over a broad range of magnetic field, they impose real limits on ARA performance, for the linear results indicate that propagation in a decreasing field will not reduce the E_z field, but rather increase the relative beam modulation. Conclusive results must await either experiments or simulations of cyclotron wave propagation in inhomogeneous fields. We are actively pursuing the latter.

A final observation of considerable interest is that the phase velocity of finite amplitude waves is very accurately given by linear theory, at least at the simulated wave strengths. Since a nonlinear frequency shift on the order of $k\Delta v_z$ plays a significant role in cylotron waves in low density beams,[8,10] measurable changes in the phase velocity should have been detectable for waves seen in the simulation. Larger amplitude waves, however, should prove a more stringent test on any nonlinear phase velocity modifications.

This work is currently being extended to larger amplitude waves, propagation in axially varying magnetic fields, and longer propagation distances. If present trends, consistent with inhomogeneous linear theory, persist, significant alterations will be needed in the design of an Autoresonant accelerator. Possible improvements may result from reshaping the acceleration section, giving smaller acceleration gradients, finding an optimum radial current profile, or employing a higher energy electron beam.

ACKNOWLEDGMENT

This work was supported under the auspices of the U. S. Department of Energy.

REFERENCES

1. M. L. Sloan and W. E. Drummond, Phys. Rev. Letters, 31, 1234 (1973).

2. R. J. Faehl and B. B. Godfrey, Phys. Rev. Letters, 40, 1137 (1978).

3. P. Sprangle, A. T. Drobot, and W. M. Manheimer, Phys. Rev. Letters, 36, 1180 (1976).

4. V. V. Velikov, A. G. Lymer,, and N. A. Khizhnyak, Sov. Phys.-Tech. Phys. Letters, 1, 276 (1975).

5. S. V. Yadavalli, to appear in J. Nuc. Instruments and Methods.

6. B. B. Godfrey, IEEE J. Plas. Sci., (Jan. 1978).

7. R. J. Faehl, B. S. Newberger, and B. B. Godfrey, submitted to Phys. Fluids.

8. H. V. Wong, I-ARA-77-U-47 (ARA-273), p. 185 (1977).

9. R. C. Davidson, Theory of Nonneutral Plasmas, W. A. Benjamin, Inc. (Reading, Massachusets), 1974.

10. G. I. Bourianoff, B. N. Moore, and B. R. Penumalli, "Computer Simulation of Linear and Non-Linear Wave Growth Phenomena," 3rd Int. Conf. on Collective Methods of Acceleration, 1978.